Responsivity improvements for a vanadium oxide microbolometer using subwavelength resonant absorbers

Evan M. Smith,[a,b,*] Janardan Nath,[a] James Ginn,[b] Robert E. Peale,[a] David Shelton[b]

[a]Department of Physics, University of Central Florida, Orlando FL 32816
[b]Plasmonics, Inc., 12605 Challenge Pkwy STE 150, Orlando FL 32826

ABSTRACT

Subwavelength resonant structures designed for long-wave infrared (LWIR) absorption have been integrated with a standard vanadium-oxide microbolometer. Dispersion of the dielectric refractive index provides for multiple overlapping resonances that span the 8-12 μm LWIR wavelength band, a broader range than can be achieved using the usual quarter-wave resonant cavity engineered into the air-bridge structures. Experimental measurements show a 49% increase in responsivity for LWIR and a 71% increase across a full waveband as compared to a similar device designed for only LWIR absorption, using a 300˚C blackbody at 35 Hz chopping rate. Increased thermal time constant due to additional mass is shown to lessen this enhancement at higher chopping rates.
Keywords: VO_x microbolometer, metamaterial absorber, MEMS, LWIR

INTRODUCTION

As the use of infrared technology has become more widespread in commercial markets, the demand for high performance, low cost detectors has increased. Uncooled microbolometers, which convert absorbed radiant power into a resistance change of an active material, are well suited to meet this demand in their ease of fabrication, efficiency and versatility. Indeed, current microbolometers achieve NETD well under 50 mK for pitch sizes of 17 μm or less [1], which is sufficient for 90% of applications. However, many select applications have no satisfactory sensing solution, such as narrow-band wavelength selectivity or polarization sensitivity. Detectors utilizing sub-wavelength metallic resonant structures, sometimes called *metamaterials*, are well suited to meet this need [2-5].

Metamaterials have gained attention in recent years for their potential to strongly absorb light at selected wavelengths [3,4]. Arrays of such structures form films that are much thinner than their resonant wavelengths. For MWIR and LWIR applications, required dimensions are still within the capability of standard UV photolithography, and dispersion within dielectric elements creates multiple resonances that span the LWIR with strong absorption [6]. The result is a highly absorbing structure that is easily configurable and requires no exotic fabrication practices. Here, we give a preliminary report of the integration of such an absorbing structure with a standard vanadium oxide (VO_x) air bridge microbolometer. Responsivity measurements are compared between devices with and without the absorbers, and a significant improvement is demonstrated, while the noise is no worse.

THEORY

Development of a similar microbolometer has been tested and reported [7], in particular with regards to sensitivity enhancement using an absorbing gold black layer [8]. The current device involves a flat architecture that addresses a mechanical stability flaw in previous efforts. In this design, nichrome (80/20 nickel-chromium) arms were chosen as the arm material as it has a low thermal conductance of 11 W/mK with a relatively high electrical conductance. The active VO_x film is encapsulated in silicon oxide to provide protection during the necessary etching steps. The bridge is formed by an isotropic silicon etch to undercut the detector, keeping the structure flat and very mechanically robust. The drawback of this approach is the lack of control in the size of the cavity under the pixel, which diminished the effect of Fabry-Perot resonance often used in detector design [9].

* *Corresponding author, email: evansmith@knights.ucf.edu*

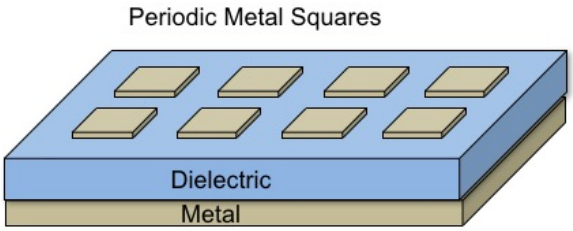

Figure 1. Schematic of the structured metamaterial absorber.

A schematic of the structured thin film absorber is shown in Figure 1. This comprises a periodic array of metal squares on a dielectric spacer over a metal ground plane. A standing-wave resonance model accurately predicts the resonant absorption wavelengths, which depend on square dimension *l*, dielectric thickness *t*, and dielectric refractive index $n(\lambda)$, according to a simple analytic formula [10]. Dependence on any other device parameter, such as periodicity, is very weak [6], and the absorption is highly localized on the individual squares, so that the main purpose of forming an array of them is to increase the fill factor. Multiple absorption bands are achieved using a dispersive dielectric such as SiO_2. Strong wideband absorption is reported for such structures which cover almost the entire LWIR region [11].

Detector responsivity is [12]

$$R_v = \frac{V_B \alpha \eta}{4G_{eff}} \frac{1}{\sqrt{1+\omega^2 \tau_{th}{}^2}} \ , \tag{1}$$

where V_B is the bias voltage, α the TCR, η the absorptance, G the thermal conductance, ω the chopping frequency, and τ_{th} the thermal time constant, which is defined as the ratio between the heat capacity and the thermal conductance as

$$\tau_{th} = \frac{C}{G} . \tag{2}$$

G is dominated by heat transfer through the arms of our air bridge structures. Responsivity increases linearly with absorption. The subject structured films have demonstrated ~90% absorption over the LWIR band [11], so that we expect integration of them with our bolometers to provide significant responsivity improvement.

The added heat capacity of an absorber will increase the thermal time constant according to Eq. 2.
The thermal conductance and heat capacity can be calculated for an ideal device based upon design geometries and materials, which gives 1.6 x 10^{-9} J/K and 1.25 x 10^{-6} W/K, respectively. By adding the absorbing film, the calculated heat capacity increases to 4.1 x 10^{-9} J/K, which increases the thermal time by a factor of 2.5.

The fabricated detectors are limited by Johnson noise [7], which is given by [12]

$$\delta V_j = \sqrt{4k_B T R \Delta f} \ , \tag{3}$$

where k_B is the Boltzmann constant, T the pixel temperature, R the electrical resistance, and Δf the measurement bandwidth. The latter is related to the measurement integration time τ_m as $\Delta f = \frac{1}{2\tau_m}$. Johnson noise is unaffected by the addition of an absorbing layer, if electrical resistance remains unchanged. However, the additional thermal mass will affect the steady-state temperature increase of the detector due to Joule heating from the applied bias. The temperature difference directly affects the temperature fluctuation noise, though this is less than 10% of the Johnson noise, so that the absorber should cause less than 10% total noise increase.

The incident power on the detector is given by [12]

$$P_i(T) = \Delta L(T) \frac{A_{BB} A_d}{r^2} F_f \tau \ , \tag{4}$$

where A_{BB} is the area of the blackbody (26.4 cm^2), A_d is the area of the detector, r is the distance from blackbody to detector, τ is the transmission of the window of the detector housing, and F_f is the incident power RMS form factor to account for the modulation of the signal. If the modulation produces a square wave with a 50% duty, then $Ff = \frac{\sqrt{2}}{Pi}$. The radiance term ΔL is determined by evaluating Planck's Law in the wavelength range of the window,

$$L = + \frac{2k^4T^4}{h^3c^2} \int_{x2}^{x1} \frac{x^3}{e^x - 1} dx \quad , x = \frac{hc}{\lambda kT} . \tag{5}$$

EXPERIMENTAL DETAILS

Figure 2 presents a schematic of the fabrication steps. First, nichrome is deposited and patterned on a thermally-oxidized silicon substrate to create the structural arms and electrical connections for the detector. Next, VO_X film is co-sputtered with gold to form the active bolometer element and patterned by UV photolithography lift-off. A layer of silicon oxide is then deposited by plasma-enhanced chemical vapor deposition (PECVD) over the surface to protect the VO_X-Au elements, to provide electrical isolation, and provide additional structural stability. The PECVD and thermal oxides are selectively co-etched to create vias to the silicon. Metal traces and bond pads are deposited and patterned by lift-off. The absorber is patterned on top of the pixel prior to the formation of the air bridge. The air bridge is achieved using an isotropic fluorinated plasma in a barrel etcher to etch a trench in the silicon underneath the pixel.

The absorber metal (200 nm Au with Ti sticking layer) and dielectric (1.3 µm evaporated silicon dioxide) layers of the absorber were deposited and patterned directly on the VO_x elements by lift-off. Then, 150-nm-thick gold squares with 5 µm lateral dimension in a 7.5 µm period two-dimensional array were patterned on the bolometers by a second lithography step. Devices without the absorber serve as reference.

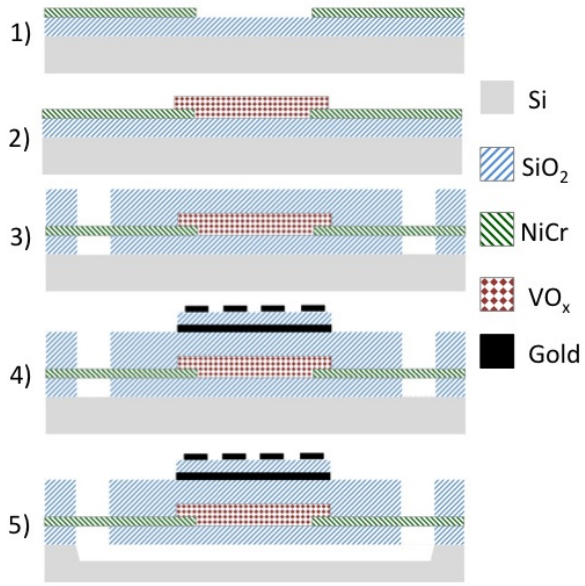

Figure 2. Schematic of the fabrication steps.

For characterization of the absorbers independent of the bolometers, the absorber structure was patterned over large areas of silicon substrates. The squares were fabricated using standard i-line UV photolithography. Reflectance spectra R were measured by Fourier Transform Infrared (FTIR) spectroscopy (Bomem DA8) using a globar source, KBr beamsplitter, and 77 K HgCdTe detector. Transmission was confirmed to be zero due to the optically thick gold ground plane on the silicon substrate, and no scattering is expected from the subwavelength squares. Hence, absorbtance $A = 1-R$.

For sensitivity measurements, the air-bridge microbolometers were wire bonded to standard chip carriers using aluminum wire onto gold bond pads. These chip carriers were placed in a vacuum box with optical access and electrical feedthroughs. The 20 mTorr vacuum pressure limited heat conduction from the bolometer. The thallium bromo-iodide (KRS-5) window on the box had a transmission of ~70% from 0.6-40 µm. This window was placed a distance r from a blackbody source (IR-301 Infrared Systems Development Corporation). An optical chopper modulated the blackbody signal. The chopper surface facing the blackbody was highly reflective to limit heating, and the surface facing the detector was blackened to limit reflections and emulate the emissivity of a blackbody at the chopper temperature. Bolometer and load resistances were matched within a 10% difference, and the circuit was biased with a voltage V_B using a low-noise DC source. The modulation in the voltage across the load resistor due to the chopped incident IR irradiance is given by

$$dV_{out} = V_B \frac{R_L}{(R_L+R)^2} dR \approx \frac{V_B}{4}\frac{dR}{R}. \quad (6)$$

The voltage drop modulation was synchronously amplified using a lock-in amplifier (Stanford Research Systems 530) with 30 ms time constant, resulting in a noise bandwidth of ~17 Hz.

Samples were tested at a blackbody temperature of 300˚C in order to achieve detector output voltages sufficiently above the instrument noise floor without the use of a read-out amplifier. While this temperature choice yields a bias towards MWIR measurements, the use of optical filters in subsequent testing eliminates this problem. Ten samples without the absorber were measured first to establish a baseline, and ten samples with the absorbers were then measured for comparison. Detectors with absorbers had an average resistance of 91.5 ± 0.6 kΩ, while detectors without patterned absorbers had an average resistance of 80.0 ± 1.2 kΩ. As the absorber is completely electrically isolated from the VO_x, it is unlikely that the application of the absorber would affect device resistance. It is far more likely that this resistance difference is indicates VO_x film variance. Resistivity measurements of witness VO_x films have shown variations up to 10% across a wafer. Signal and noise voltages for both samples were measured as a function of chopping frequency, applied bias voltage, and incident power spectral bandwidth.

The detector noise was measured in a manner described in the ASTM standard for NETD measurements [13]. The incident power from the blackbody source was blocked by a shield, which is highly reflecting on the side facing the blackbody so as to not absorb heat, and which is highly emissive on the side facing the detector. The signal voltage with the blackbody blocked is the noise.

RESULTS

Fig. 3 presents SEM images of detectors with and without the absorbers. The top image of the detectors without absorbers is taken from a separate wafer designed with a higher fill factor, but in every other regard the design is identical to the detectors tested in this work. The top-layer squares of the absorber cover the central region of the detector with high spatial uniformity, although squares near the edges are often smaller or deformed as a result of the patterning process. The squares are also more rounded than originally designed. The undercut depth significantly exceeds the quarter-wave dimension needed for Fabry-Perot resonant absorption, so that the applied absorbers are expected to account for much of the absorbed IR.

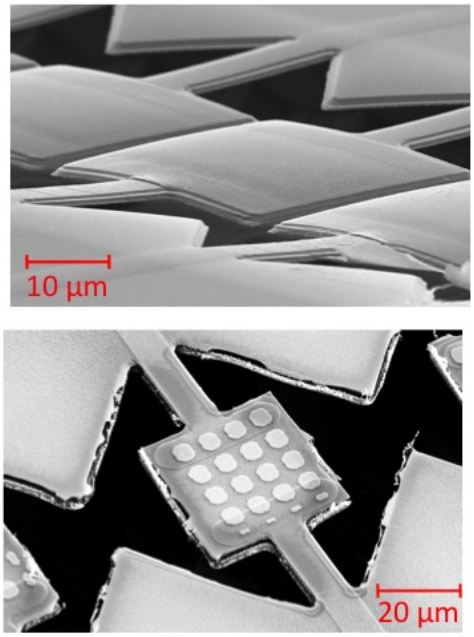

Figure 3. Air bridge detector without (top) and with (bottom) the added absorbing structures.

Measured reflectance spectra for the large area absorber films are plotted in Figure 4. Multiple absorption bands appear at the indicated wavelengths. The average absorptance over the LWIR is ~80%. Average absorptance across the MWIR is ~45%.

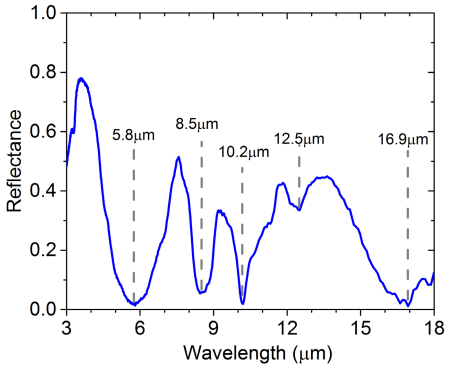

Figure 4. Reflectance spectra of reference absorber array measured by FTIR. Reflectance minima (absorption peaks) are labeled.

Bolometer testing conditions and results are presented in Table 1. For each set of conditions, measurements for the 10 different elements were averaged. Applied bias was 1.0 V in each case. "Full" bandwidth means the measurement was performed without an optical filter, so the incident power spectrum depended only on the blackbody spectrum, atmospheric transmission, and the KRS-5 transmittance. For "LWIR" bandwidth, an anti-reflection-coated germanium long pass optical filter was used (Edmund Optics 68656), which has a spectral window of about 7.6 - 14.6 µm. The lock-in time constant was 30 ms, giving a measurement bandwidth f of ~17 Hz.

The responsivity was highest at 35 Hz modulation frequencies, which is acceptable for video frame rates. The responsivity was consistently higher with an absorber than without. For 35 Hz modulation frequency, the detectors with absorbers showed a 71% increase in responsivity, but only a 56% increase at 100 Hz. This is likely due to the increase in thermal time constant with the additional mass of absorber. With LWIR filter, responsivity improvement at 35 Hz drops to 49%. The higher responsivity for the full band measurements is largely due to increased absorption outside of the LWIR bandwidth.

Modulation Frequency [Hz]	Bandwidth	Detector	Average Responsivity [V/W]	Average Noise Voltage [μV]
35	Full	Absorber	1399 ± 36	0.67 ± 0.37
		No Absorber	817 ± 21	0.49 ± 0.29
100	Full	Absorber	656 ± 14	0.73 ± 0.35
		No Absorber	420 ± 14	0.49 ± 0.25
35	LWIR	Absorber	2171 ± 51	0.42 ± 0.16
		No Absorber	1457 ± 36	0.33 ± 0.17

Table 1. Data averaged over 10 detectors with and without the absorbing structure.

The measured noise was larger for devices with the absorbers, but the increase was within the statistical uncertainty. With a resistance of 80-90 kΩ, the Johnson noise for measured devices should approximately 200 nV by Eq. 30, which is 2-3 times lower than presented in Table 5. While previous experiments for similar devices have shown a presence of high 1/f noise, the data do not support this conclusion, as noise is of similar magnitude at 35 Hz and at 100 Hz modulation frequency.

5. SUMMARY

We have demonstrated the integration of a thin-film sub-wavelength structured absorber onto a vanadium oxide microbolometer. Strong increase in responsivity resulted due to improved absorption. Importantly, the absorption band is much more easily tunable by design than can be done with Fabry-Perot resonant cavities. The device can be entirely patterned by photolithography and requires no exotic steps or materials. While detector speed is decreased, as limited by the modest increase in thermal time constant, the rate is sufficient for standard video frame rates.

ACKNOWLEDGMENTS

This research was supported by a grant from the US Army Research Labs (ARL) SBIR program. We would also like to acknowledge the support and assistance from Mr. Guy Zummo, Mr. Ed Dein and Prof. Kevin Coffey. We would like to thank Dr. Glenn Boreman for the use of optical filters. Also thanks to help from Alvar Rodriguez for wire bonding assistance, Pedro Figueiredo for assistance in device testing and FTIR support.

REFERENCES

[1] Skidmore, G.D., Han, C.J., Li, C., "Uncooled microbolometers at DRS and elsewhere through 2013," Proc. SPIE 9100, 910003 (2014).
[2] Liu, N., Mesch, M., Weiss, T., Hentschel, M., and Giessen, H. "Infrared Perfect Absorber and Its Application As Plasmonic Sensor," Nano Lett. 10(7), 2342-2348 (2010).
[3] Watts, C.M., Liu, X., and Padilla, W. J. "Metameterial Electromagnetic Wave Absorbers," Adv. Mater. 24(23), 98-120 (2012).
[4] Ogawa, S., Komoda, J., Masuda, K., and Kimata, M. "Wavelength Selective Wideband Uncooled Infrared Sensor Using a Two-dimensional Plasmonic Absorber," Proc. SPIE 8704, 8704181-8704186 (2013).
[5] Zhu, H., F. Yi, and E. Cubukcu, "Nanoantenna absorbers for thermal detectors," Photonics Technology Letters, IEEE, 24(14): p. 1194-1196 (2012).
[6] Nath, J., Panjwani, D., Khalilzadeh-Rezaie, F., Yesiltas, M., Smith, E. M., Ginn, J. C., Shelton, D. J., Hirschmugl, C., Cleary, J. C., and Peale, R. E., "Infra-red spectral microscopy of standing-wave resonances in single metal-dielectric-metal thin-film cavity" Proc. SPIE OP101-57, 95442M-95442M, 2015.
[7] Smith, E. M., Ginn, J.C., Warren, A.P., Long, C.J., Panjwani, D., Peale, R.E., Shelton, D.J. "Linear Bolometer array using a high TCR VO_x-Au film," Proc. SPIE 9070, 90701Z (2014).
[8] Smith, E.M., Panjwani, D., Ginn, J., Warren, A.P., Long, C., Figuieredo, P., Smith, C., Nath, J., Perlstein, J., Walter, N., Hirschmugl, C., Peale, R.E., Shelton, D., "Dual band sensitivity enhancements of a VOx microbolometer array using a patterned gold black absorber," Appl. Opt. 55, 2071-2078 (2016).
[9] Niklaus, F., Vieider, C., and Jakobsen, H., "MEMS-Based Uncooled Infrared Bolometer Arrays-A Review," Proc. SPIE 6836, 68360D (2007).

[10] Nath, J., Modak, S., Rezadad, I., Panjwani, D., Rezaie, F., Cleary, J. W., and Peale, R. E., "Far-infrared absorber based on standing-wave resonances in metal-dielectric-metal cavity" Optics Express, 20366-20380, 23(16), 2015.
[11] Nath, J., Maukonen, D., Smith, E., Figueiredo, P., Zummo, G., Panjwani, D., Peale, R. E., Boreman, G., Cleary, J. C., and Eyink, K., "Thin-film, wide-angle, design-tunable, selective absorber from near UV to far infrared," Proc. SPIE 8704, 127 (2013).
[12] Dereniak, E. L. and Boreman, G. D., [Infrared Detectors and Systems], John Wiley and Sons, New York, (1996).
[13] ASTM Standard E1543-00 (2012), "Standard Test Method for Noise Equivalent Temperature Difference of Thermal Imaging Systems," ASTM International, West Conshohocken, PA, 2012, DOI: 10.1520/E1543-00R11, www.astm.org.